CellPress

One Earth

Article

Oxidation of commercial antioxidants is driving increasing atmospheric abundance of organophosphate esters: Implication for global regulation

Qifan Liu,[1,3,4,16,*] Runzeng Liu,[2,4,16] Xianming Zhang,[5,16] Wenlong Li,[6,7,16] Tom Harner,[7] Amandeep Saini,[7] Hanyang Liu,[1] Fange Yue,[1] Lixi Zeng,[8] Ying Zhu,[9] Changyue Xing,[9] Li Li,[10] Patrick Lee,[7] Shengrui Tong,[11] Weigang Wang,[11] Maofa Ge,[11]

(Author list continued on next page)

[1]Anhui Key Laboratory of Polar Environment and Global Change, Department of Environmental Science and Engineering, University of Science and Technology of China, Hefei 230026, China
[2]Shandong Key Laboratory of Environmental Processes and Health, School of Environmental Science and Engineering, Shandong University, Qingdao 266237, China
[3]State Key Laboratory of Fire Science, University of Science and Technology of China, Hefei 230026, China
[4]Department of Chemistry, University of Toronto, Toronto, ON M5S 3H6, Canada
[5]Department of Chemistry and Biochemistry, Concordia University, 7141 Sherbrooke Street West, Montreal, QC H4B 1R6, Canada

(Affiliations continued on next page)

SCIENCE FOR SOCIETY Organophosphate esters (OPEs), a group of synthetic chemicals widely used as flame retardants, are ubiquitously present in the global environment, including urban, rural, and polar regions. Recent studies indicate that OPEs can harm ecosystems and human health, including increased cancer risks. In response to the potential environmental and health risks posed by OPEs, seven states in the United States and the European Union have issued regulations on OPEs, including limiting or prohibiting their use in commercial products. Our results suggest that OPEs are not only emitted from known sources such as flame retardants but can also be produced when other commercial chemicals are transformed in the air. This implies that existing OPE regulations designed to limit OPE pollution may not be sufficient. Our study emphasizes the need for more comprehensive policies to control environmental OPEs.

SUMMARY

Organophosphate esters (OPEs) are chemicals of global concern due to their adverse effects on humans and the environment. Environmental OPEs are thought to originate via direct emissions; therefore, existing OPE regulations focus on limiting the use of certain OPEs in commercial products. Here, we present experimental and field evidence that OPEs can also be formed from reactions between atmospheric ozone and organophosphite antioxidants (OPAs; a group of mass-produced chemicals), representing an important indirect source of environmental OPEs. We demonstrate that tris(2,4-di-*tert*-butylphenyl) phosphate (TDtBPP), a novel OPE formed from OPA chemical transformation, is globally distributed from megacities to the Antarctic and Arctic, with concentrations in Arctic air significantly increasing since 1994. Furthermore, TDtBPP is substantially more persistent in the environment and may pose a higher risk relative to the traditional OPEs. These results highlight the importance to consider chemical transformations of contaminants in developing environmental regulations to protect environmental health.

INTRODUCTION

Commercial chemicals play a fundamental role in daily life, but some can cause adverse impacts on the environment and humans,[1] making regulation of harmful chemicals an essential step in achieving the United Nations' Sustainable Development Goals.[2] Therefore, chemicals of concern should be minimized and replaced as much as possible, as noted in the "Chemicals

Jianjun Wang,[12,13] Xiaoguo Wu,[14] Cassandra Johannessen,[5] John Liggio,[7] Shao-Meng Li,[15] Hayley Hung,[7,*] Zhouqing Xie,[1,3,*] Scott A. Mabury,[4,*] and Jonathan P.D. Abbatt[4,17,*]

[6]College of the Environment and Ecology, Xiamen University, Xiamen 361102, China
[7]Air Quality Processes Research Section, Environment and Climate Change Canada, Toronto, ON M3H 5T4, Canada
[8]Guangdong Key Laboratory of Environmental Pollution and Health, School of Environment, Jinan University, Guangzhou 511443, China
[9]State Environmental Protection Key Laboratory of Environmental Health Impact Assessment of Emerging Contaminants, School of Environmental Science and Engineering, Shanghai Jiao Tong University, Shanghai 200240, China
[10]School of Public Health, University of Nevada Reno, Reno, NV 89557, USA
[11]State Key Laboratory for Structural Chemistry of Unstable and Stable Species, CAS Research/Education Center for Excellence in Molecular Sciences, Institute of Chemistry, Chinese Academy of Sciences, Beijing 100190, China
[12]Third Institute of Oceanography, Ministry of Natural Resources, Xiamen 361005, China
[13]State Key Laboratory of Marine Resource Utilization in South China Sea, Hainan University, Haikou 570228, China
[14]College of Environmental Science and Engineering, Anhui Normal University, Wuhu 241002, China
[15]State Key Joint Laboratory of Environmental Simulation and Pollution Control, College of Environmental Sciences and Engineering, Peking University, Beijing 100871, China
[16]These authors contributed equally
[17]Lead contact
*Correspondence: liuqifan@ustc.edu.cn (Q.L.), hayley.hung@ec.gc.ca (H.H.), zqxie@ustc.edu.cn (Z.X.), scott.mabury@utoronto.ca (S.A.M.), jonathan.abbatt@utoronto.ca (J.P.D.A.)
https://doi.org/10.1016/j.oneear.2023.08.004

Strategy for Sustainability" recently adopted by the European Union (EU).[3] Organophosphate esters (OPEs) are chemicals of emerging concern (CECs) that have gained significant international attention.[4] They are extensively used as flame retardants and plasticizers in consumer products and building materials.[4] The global production of OPEs has increased substantially in recent years as a result of the phase-out of traditionally used brominated flame retardants.[5] However, recent evidence indicates that OPEs may exert negative effects on ecosystems (e.g., destabilize the ecological balance) and human health (e.g., increase the risk of cancer).[5,6] The ubiquitous presence of OPEs in the global environment emphasizes their potential for widespread environmental and human health risks,[6,7] suggesting that OPEs are not necessarily an appropriate substitute for brominated flame retardants.[5]

In response to increasing public concerns over OPE exposures, authorities in the United States, Europe, and Canada have begun to evaluate and regulate certain OPEs. For example, under the Toxic Substances Control Act, in 2019, the United States Environmental Protection Agency proposed two widely used OPEs (TCEP [tris(2-chloroethyl) phosphate] and TPHP [triphenyl phosphate]) as high-priority chemicals that need to be scrutinized.[8] Although OPEs are presently at the risk evaluation stage at the federal level, seven states in the United States (e.g., California, Maryland, and Minnesota) have issued their own regulations, such as limiting the use of some OPEs in children's products and residential furniture (Figure S1; Table S1). Similarly, EU has banned the use of halogenated OPEs in electronic display enclosures and stands,[9] effective March 2021. Recently, the Government of Canada proposed the implementation of regulatory measures to minimize the use of aryl OPEs in consumer products.[10]

The existing OPE regulations point to the prohibition or restriction on the use of OPEs in commercial products. This is because environmental OPEs are believed to originate only from the volatilization, abrasion, and leaching of OPE-containing products, representing a direct emission source.[11] Recent studies found that a novel OPE [tris(2,4-di-*tert*-butylphenyl) phosphate (TDtBPP)] was present in indoor dust and ambient particles in megacities,[12–14] which was proposed as a possible transformation product of tris(2,4-di-*tert*-butylphenyl) phosphite (TDtBPPi; a widely used organophosphite antioxidant [OPA] in the manufacturing of plastics).[13,14] Although few studies observed the OPA-derived OPEs in urban regions, no information is available regarding their occurrence and temporal trends in remote areas (Arctic and Antarctic). Note that Arctic contaminant monitoring is of critical importance for chemical regulation. First, the observation of a contaminant in the remote Arctic serves as evidence for its potential for long-range environmental transport, which warrants its nomination as a candidate for listing under the Stockholm Convention on Persistent Organic Pollutants (POPs) deemed for global control.[15,16] Second, long-term analysis of contaminants in the Arctic provides a critical approach to evaluating the effectiveness of international chemical control strategies.[17,18] For example, the declining trends of some POPs in the Arctic air reflect the successful efforts of the Stockholm Convention in supporting existing regulations and further reducing the presence of POPs in the environment since its implementation in 2004.[18]

In addition to the knowledge gap in environmental monitoring, the transformation pathway from OPAs to OPEs and the environmental hazards (persistent, biotransformation, and toxic properties) of novel OPEs remain largely unknown. Given that environmental monitoring and risk assessment play key roles in policymaking related to contaminants control, these two knowledge gaps hinder a comprehensive assessment of the global impact of OPA transformation on environmental OPEs, which is essential for the ongoing OPE regulatory development in the United States, EU, and Canada.

Here, we combine global (Arctic, Antarctic, and megacities) field measurement, laboratory experiments (OPA→OPE chemical transformation experiments and OPE biotransformation experiments), and *in silico* modeling (persistence and toxic properties of novel OPEs formed from OPA transformation) to study the global impact of OPA transformation chemistry on environmental OPEs. This work provides an improved fundamental

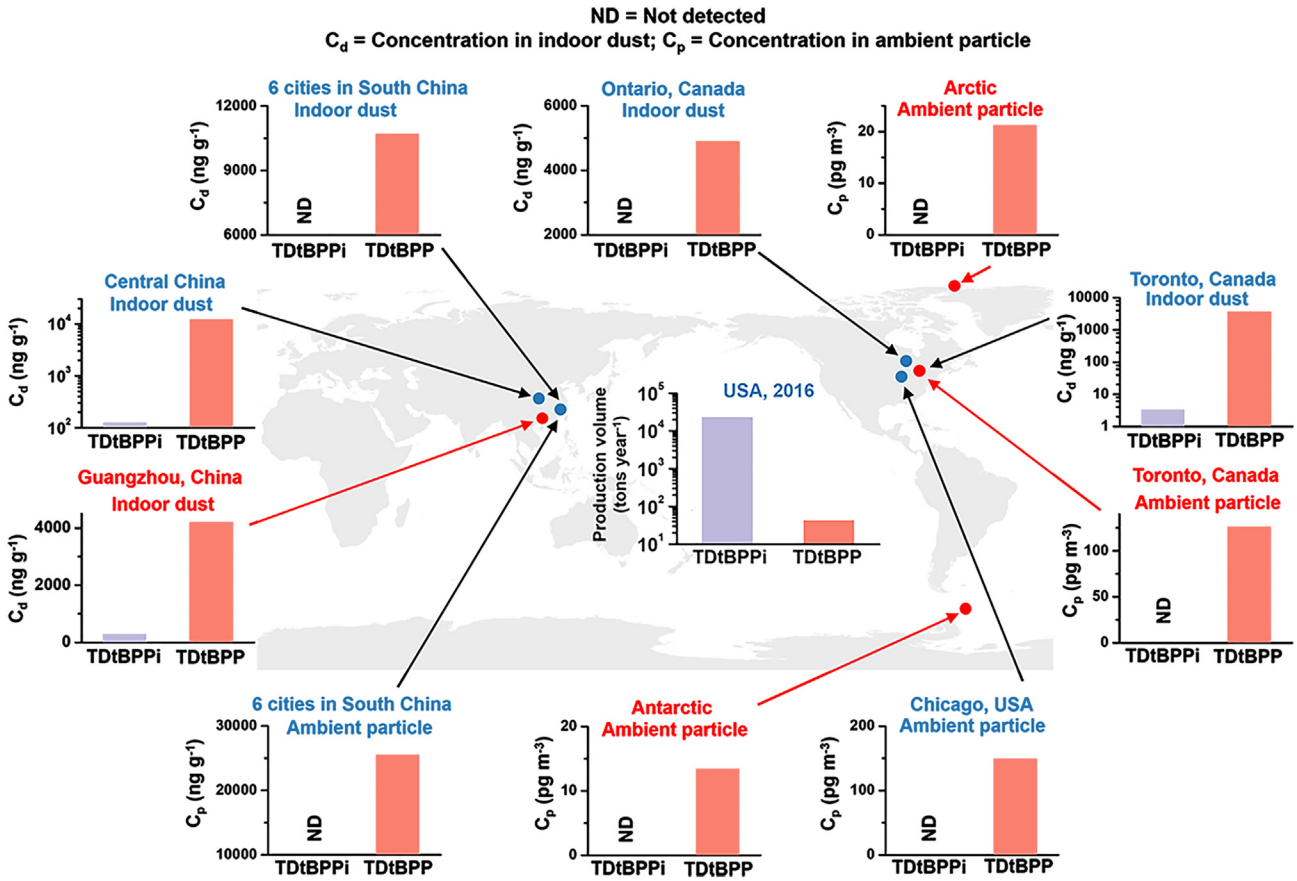

Figure 1. Global distribution of TDtBPPi and TDtBPP

Shown are median concentrations (ng g^{-1} or pg m^{-3}) in indoor dust and ambient particles. Source of data: ambient particle in Chicago, Illinois, USA, and indoor dust in Ontario, Canada[12]; indoor dust in Toronto, Ontario, Canada[13]; indoor dust and ambient particle in six cities (Guangzhou, Shenzhen, Zhuhai, Foshan, Zhongshan, and Maoming) in South China[19]; indoor dust (from e-waste dismantling workshops) in Central China[20]; production volume of the OPA TDtBPPi and the OPE TDtBPP in the United States (Table S2). The ambient particle data in the Arctic (samples collected in January–December 2018), Antarctic (samples collected in January 2020–January 2021), and Toronto (samples collected in January–February 2018) and indoor dust data in Guangzhou, China (samples collected in July–August 2021) are obtained from this work (shown in red dots in the map). The indoor dust results for Central China and Toronto are given in log scale. TDtBPP, tris(2,4-di-*tert*-butylphenyl) phosphate; TDtBPPi, tris(2,4-di-*tert*-butylphenyl) phosphite.

understanding of the source and environmental and human health impacts of OPEs, particularly for those formed from OPA transformation. These results have significant implications for OPE regulatory development, as discussed below.

RESULTS AND DISCUSSION

Global (Arctic, Antarctic, and megacities) field measurements

To investigate the potential for the presence of OPA-derived OPEs in polar regions, we analyzed ambient particle samples collected in the Arctic and Antarctic. Note that it is difficult to evaluate the impact of OPA transformation on environmental OPEs if the investigated OPEs are high-production volume chemicals themselves (i.e., likely having a strong, direct emission source). For that reason, the analysis is focused on TDtBPPi and TDtBPP given their large difference in production volumes, i.e., the production volume of the OPA TDtBPPi in the United States (up to 2.3 × 10^4 tons year^{-1}) is 530 times higher than that of OPE TDtBPP (43 tons year^{-1}; Table S2). Despite having such a high production volume, TDtBPPi is not detected in the Arctic and Antarctic (Figure 1). Conversely, TDtBPP, which has a much lower production volume than TDtBPPi, was detected in both regions in 2018–2021, with median concentrations of 21 and 13 pg m^{-3}, respectively, in the Arctic and Antarctic.

In addition to the Arctic and Antarctic measurements, to give a full picture of the presence of TDtBPPi and TDtBPP in the outdoor and indoor environment, we also analyzed ambient particle and indoor dust samples collected in various megacities across the globe. The analyzed data include our TDtBPPi and TDtBPP measurement data from Canada and China and literature data from the United States, Canada, and China.[12,13,19,20] Similar to the scenario in the Arctic and Antarctic, TDtBPPi is detected in only 37% of these megacity samples, with concentrations orders of magnitudes lower than TDtBPP. As shown in Figure 1 and Table S3, TDtBPP is globally distributed in both the urban outdoor air (e.g., Chicago and Toronto, ON, Canada; 126–149 pg m^{-3}) and the indoor dust collected across nine cities (e.g.,

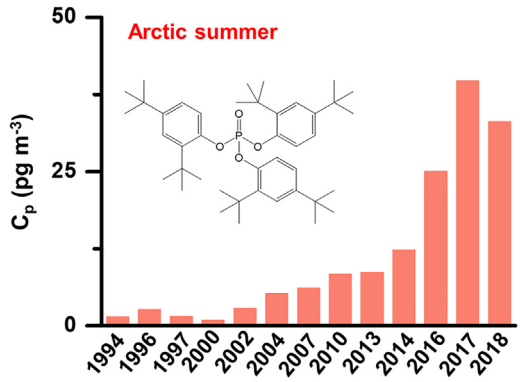

Figure 2. Increased concentration of the OPE TDtBPP in the Arctic air over the past 24 years (1994–2018)

Samples from summer (June–August) were collected from the Alert Global Atmosphere Watch Observatory, Nunavut, Canada.[21] The concentrations of TCEP, TCPP, and TPHP in the Arctic air over the past 24 years are shown in Figure S3. C_P, median concentration in the ambient particle (pg m^{-3}).

Toronto and Guangzhou, China; up to 1.1 × 10^4 ng g^{-1}) worldwide, with detection frequencies of 95%–100%.

The striking inconsistency between the production volumes and the measured concentrations of TDtBPPi and TDtBPP around the world provides potential evidence for the transformation of TDtBPPi to TDtBPP in the global environment. Furthermore, among all the environmental samples (ambient air and indoor dust samples) collected from different sampling sites (polar regions and megacities), the concentration of TDtBPP (a novel OPE that is not monitored in routine atmospheric monitoring networks[7]) is higher than or comparable with that of well-studied, traditional OPEs (including TCEP; Figure S2), despite its significantly lower production volume compared with the traditional OPEs (Table S2). In summary, the TDtBPPi→TDtBPP example illustrates the potential importance of OPA transformation in the formation of environmental OPEs.

Increasing levels of TDtBPP in Arctic air

As the first report of the presence of TDtBPP in the Arctic and Antarctic environments, our work suggests that environmental pollution arising from OPA transformation is a global issue. To assess whether the OPA-transformation-induced pollution is an emerging or long-lasting environmental issue, we analyzed the archived extracts from Arctic air samples collected over the past 24 years, from 1994 to 2018, under Canada's Northern Contaminants Program.[21] TDtBPP was detected in all the Arctic samples, with median concentrations increasing from 1.4 pg m^{-3} in the summer of 1994 to 33 pg m^{-3} in the summer of 2018 (Figure 2). The dramatic increase of TDtBPP concentration in the Arctic air is likely related to the rapid growth of plastics production (leading to the increasing use of antioxidants) over the past two decades,[22] reflecting a strong impact of chemical emissions from plastics on the Arctic environment.

Further analysis reveals a seasonality associated with the formation of TDtBPP. In particular, among the Arctic air samples, the TDtBPP concentrations were two times higher in summer than in winter (Figure S3A). The observed seasonal contrast can be explained by the "transformation chemistry" hypothesis for OPAs (including TDtBPPi), as discussed below.

Transformation mechanism and kinetics for OPAs upon ozone oxidation

A full understanding of the environmental behavior of OPA-derived OPEs (including TDtBPP) requires knowledge of the chemical transformation mechanism of OPAs. Previous studies suggest that OPEs can be formed through photo-transformation and O_2 oxidation of OPAs.[14,23,24] In addition to these two transformation mechanisms, here we propose a new mechanism: transformation of OPAs can lead to the formation of OPEs via heterogeneous interactions with atmospheric ozone (O_3) in the dark.

The importance of such transformations for OPAs was studied by exploring the heterogeneous reaction kinetics and chemical mechanisms of OPAs coated on glass slides (estimated average coating thickness, ~1 nm) upon exposure to gas-phase O_3 (Figure S4). The OPAs investigated include tris(2-chloroethyl) phosphite (TCEPi), triphenyl phosphite (TPHPi), and TDtBPPi, representing chlorinated, aryl, and the most frequently used OPAs, respectively. As shown in Figure 3A, the amount of TCEPi decreased by 56% when exposed to 260 ppb of O_3 for 150 min, indicating that the chemical transformation of TECPi occurred. A similar chemical change was observed for TPHPi and TDtBPPi (Figures 3B and 3C). The decrease of the mass of OPAs was solely caused by O_3 reaction (and not by O_2 or water reaction), because control experiments demonstrated that the presence of O_2 and water vapor had no impact on the decay of OPAs within the experimental period (Figure S5). Interestingly, the heterogeneous reaction rate constant (k) for the loss of TDtBPPi ([3.3 ± 0.2] × 10^{-15} cm^3 molecule^{-1} s^{-1}) is orders of magnitude higher than those of TCEPi and TPHPi ([1.5 ± 0.1] × 10^{-17} and [2.3 ± 0.1] × 10^{-16} cm^3 molecule^{-1} s^{-1}, respectively; Figure 3D; Table S4). The difference in the reactivity of OPAs is due to their structural differences, whereas all OPAs may undergo O_3 reaction to form OPEs (see the next paragraph).

Although the amount of OPAs decreased considerably with increasing O_3 exposure time, the corresponding OPEs were simultaneously formed (Figure S6), with formation yields of up to 92% ± 4% (Figure 3E). The high formation yield of OPEs is consistent with a previous study on O_3–triphenylphosphine (R_3P) reactions in 2,4-dimethylhexane solution, which found that only triphenylphosphine oxide (R_3P = O) was formed, with no side reactions.[25] The OPA oxidation mechanism likely begins with O_3 addition to the phosphorous center of an OPA molecule, producing an "OPA–O_3 intermediate," which subsequently transforms to OPE with the loss of O_2 (Figure 3F). In this case, O_3 favors phosphorous centers that have a high density of polarizable electrons. Given the electron-donating effect of butylphenyl and phenyl groups, and the electron-withdrawing effect of chlorine, it is expected that TDtBPPi and TPHPi possess higher reactivity compared with TCEPi (having a relatively lower electron density at the phosphorous center; Figure S7), explaining the kinetic results in Figure 3D. Together, these results imply that all OPAs may undergo O_3 reactions to form OPEs.

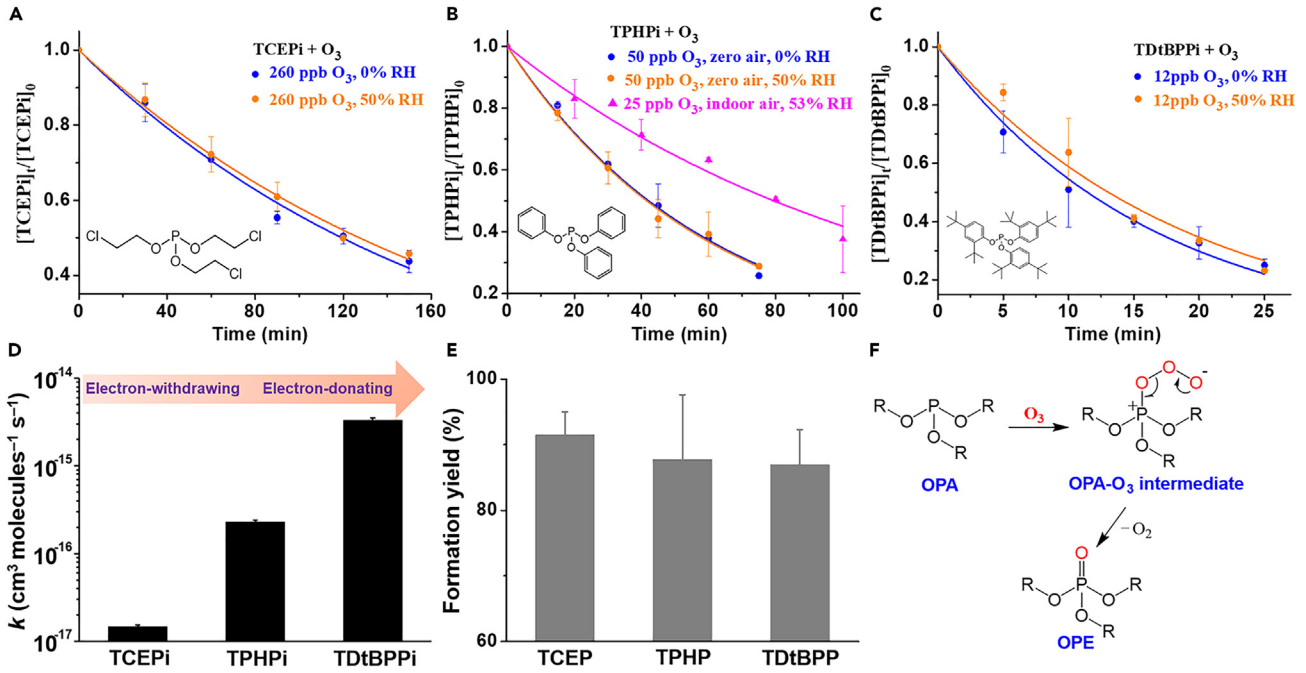

Figure 3. Experimental results for heterogeneous O_3–organophosphite antioxidant (OPA) reactions

(A–C) Mass fractions of (A) TCEPi [tris(2-chloroethyl) phosphite], (B) TPHPi (triphenyl phosphite), and (C) TDtBPPi coated on cover glasses (coating thickness ~1 nm) as a function of O_3 exposure time at 298 K and 0%–53% relative humidity (RH). $[OPA]_0$ and $[OPA]_t$ represent the initial mass of OPA and the mass of OPA at a given O_3 exposure time, respectively. Different O_3 concentrations were used for different OPA experiments because of their different reactivities.

(D) Heterogeneous second-order reaction rate constants k (cm^3 $molecule^{-1}$ s^{-1}) of OPAs.

(E) Formation yields (%; by mol) of organophosphate esters (OPEs) during O_3–OPAs reactions. O_3 concentrations are shown in (A)–(C). Error bars represent the standard deviation of formation yields obtained from O_3 oxidation experiments.

(F) Proposed O_3 oxidation mechanism for OPAs. The kinetic results indicate that for a given OPA, its reactivity is independent of the RH conditions (0% or 50% RH) and air conditions (similar kinetics for O_3 in zero air or O_3 in genuine indoor air; Table S4).

To our knowledge, this is the first study that demonstrates the fast heterogeneous reactivity of OPAs toward O_3. The newly recognized heterogeneous O_3 oxidation mechanism provides important insights into the transformation of OPAs to OPEs in the environment, as outlined below.

1. With the measured O_3 reaction rate constants in Figure 3D, a picture of the atmospheric lifetime for the free, surface-bound OPA molecules emerges. The estimated lifetimes for the three OPAs investigated here are exceedingly short (0.1–77 h; Figure S8) upon exposure to indoor and outdoor O_3 (10–30 ppb).[26,27] Consequently, most surface-bound OPAs will transform to OPEs around their emission sources (e.g., megacities). This is consistent with the TDtBPPi results shown in Figure 1. Given the rapid O_3 oxidation kinetics, the rate-determining step for the transformation of OPAs to OPEs will likely be the rate of release of OPAs within plastics to the environment, via either plastics abrasion (emission of OPA-containing microplastics) or molecular diffusion (OPAs diffuse to the surface of plastics).
2. Our findings may help to better illustrate previous experimental data. As mentioned above, a previous study suggested that O_2 was the key oxidant to oxidize OPA based upon open-air experiments.[14] However, the current results clearly indicate that O_2 has no impact on OPA transformation, and O_3 is the key oxidant to induce the oxidation process. This suggests that the oxidant in the previous open-air (containing both O_2 and O_3) experiments should be O_3 and not O_2.[13,14]
3. Indoors, O_3 oxidation chemistry is likely to be the dominant process, given the ubiquitous presence of O_3 in indoor air and the low level of light intensity indoors (compared with outdoors).[28] Outdoors, in the daytime, environmental OPAs can convert to OPEs through photo-transformation and O_3 oxidation. Although, in the nighttime outdoors, the "O_3 oxidation" pathway may play an essential role in the OPA transformation process.
4. As mentioned earlier, the TDtBPP concentrations in the Arctic are higher in summer than in winter. Atmospheric O_3 concentrations in summer are generally higher than those in winter, as observed in many sites on the continent.[29–31] The seasonality for TDtBPP may be caused by the higher levels of O_3 and strong light intensity in summer (in cities), which facilitate the transformation reactions of TDtBPPi. Another possible reason is that higher temperatures in summer (relative to winter) promote the release of TDtBPPi into the air from commercial products. Also, the reaction rate of TDtBPPi may increase with increased temperature. These factors can enhance the formation of TDtBPP.

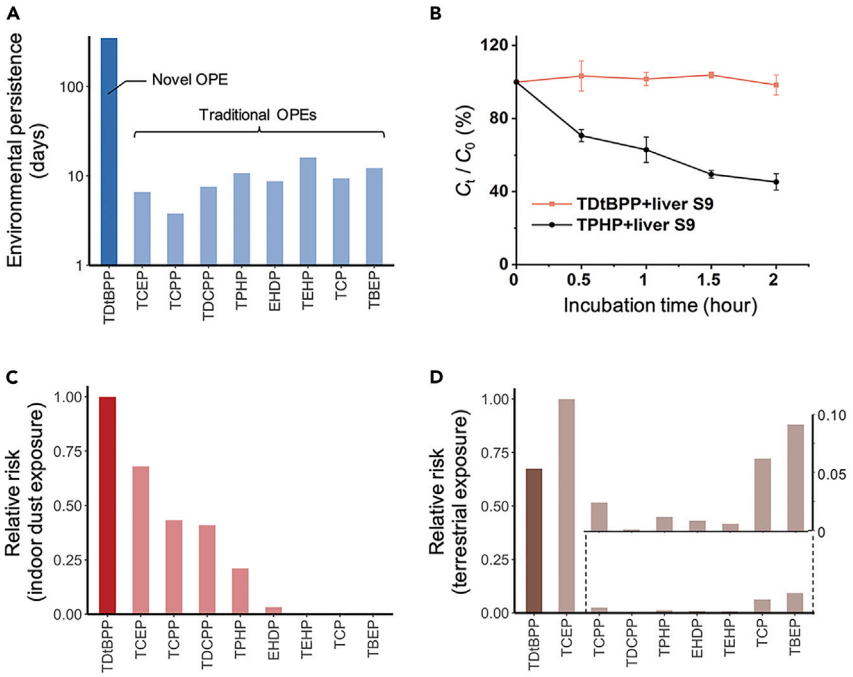

Figure 4. Comparisons of TDtBPP with traditional OPEs for their persistence and relative risks

Novel OPE (dark color bars): TDtBPP. Traditional OPEs (light color bars): TCEP, TCPP (tris(2-chloroisopropyl) phosphate), TDCPP (tris(1,3-dichloro-2-propyl) phosphate), TPHP (triphenyl phosphate), EHDP (2-ethylhexyl diphenyl phosphate), TEHP (tris(2-ethylhexyl) phosphate), TCP (tricresyl phosphate), and TBEP (tris(2-butoxyethyl) phosphate).

(A) The overall environmental persistence (days) estimated using the OECD screening model.[32]

(B) *In vitro* biotransformation results for TDtBPP and TPHP in rat liver S9. C_0 and C_t represent the initial OPE concentration and the measured OPE concentration at a given incubation time, respectively.

(C) The relative risk associated with human exposure to indoor dust.

(D) The relative risk associated with terrestrial environmental exposures. The relative risks were calculated as the exposure-to-toxicity ratios scaled to the highest values among all the OPEs. The indoor exposures were calculated with measured OPE concentrations in indoor dust from Toronto (Figure S2). The terrestrial food web exposures were calculated with the PROTEX model[33] constrained with measured OPE concentrations in the air of Chicago (Figure S2).

Hazard and risk assessment

Environmental persistence

The ubiquitous global occurrence of TDtBPP and its long-term observation record in the Arctic (Figures 1 and 2) are particularly concerning given the *in silico* and experimental evidence of hazards and risks illustrated in Figure 4. Figure 4A shows the overall environmental persistence (the total resistance to degradation across all environmental media, including air, water, and soil) of the novel TDtBPP and eight traditional OPEs estimated using the OECD (Organization for Economic Co-operation and Development) screening model.[32] TDtBPP is estimated to be 22–92 times more persistent in the environment than the traditional OPEs. Similarly, the estimated characteristic travel distance in air for TDtBPP is also higher than the traditional OPEs (Figure S9C). The greater persistence of TDtBPP is due to a higher fraction present in the water and soil wherein TDtBPP degrades more slowly than the traditional OPEs (see Figure S9 and Note S1).

Biotransformation of OPEs

In addition to the higher resistance to environmental degradation, TDtBPP is also more resistant to biotransformation than the traditional OPEs. Figure 4B presents our *in vitro* biotransformation experimental results for TDtBPP and TPHP. After 2 h of incubation with the rat liver S9 (supernatant fraction of rat liver homogenate widely used for metabolism studies), 55% of TPHP had been metabolized. By contrast, no significant decrease in the TDtBPP concentration was observed within the experimental period. This is likely attributed to the hindrance effect of the butyl substituents on each aryl group of TDtBPP.

The distinct fate of TDtBPP was further confirmed with *in vivo* rat studies. TPHP can be significantly metabolized, with high concentrations of diphenyl phosphate (DPHP; a biotransformation product) detected in both rat urine and feces (up to 4.3 × 10^4 ng mL^{-1} and 1.6 × 10^4 ng g^{-1}, respectively; see Figure S10 and Note S2). However, after TDtBPP administration, very low levels of bis(2,4-di-*tert*-butylphenyl) phosphate (BDtBPP) were detected in rat feces ($\leq$14 ng g^{-1}; Figure S10), whereas no BDtBPP was detected in rat urine. The ratio of DPHP/TPHP was 1.1 in liver, whereas the ratio of BDtBPP/TDtBPP was only 0.001 in rat liver, clearly demonstrating the high resistance to biotransformation of TDtBPP. The high stability of TDtBPP will contribute to its accumulation in rats, as verified by analyzing the rat livers 24 h after chemical administration. The concentration ratio of liver/blood was 19 and 590 for TPHP and TDtBPP, respectively, indicating that TDtBPP is more liable to deposit in liver (Figure S10). The high deposition of TDtBPP in liver may cause potential toxic effects.

The high persistence of TDtBPP in the environment and organisms is concerning. As proposed by a recent study, high persistence alone should be a major cause of concern for chemical management.[34] This is because the environmental concentrations of persistent chemicals may eventually reach thresholds for toxic effects to occur, thus posing risks to the global environment and human health. More importantly, once negative effects are identified for these chemicals, it may take decades to reverse contamination because of their persistent nature, as with chlorofluorocarbons (CFCs) and dichloro-diphenyl-trichloroethane (DDT).[35,36]

Risk evaluation

Figure S11 illustrates that the toxicity (median lethal dose of rat oral exposure) of TDtBPP is not lower than that of traditional OPEs such as TCEP. Based upon the toxicity of OPEs and their exposure estimated from environmental concentrations, we further evaluated the risks of OPEs under two different exposure scenarios. The first scenario considers human exposure to indoor dust based on data from Toronto (Figure S2). The results

indicate that the relative risk (RR) associated with indoor dust exposure to TDtBPP is higher or comparable with those of the eight traditional OPEs (Figure 4C). Due to the lack of experimental data to derive exposures of TDtBPP via other pathways (inhalation and dermal absorption), we estimated the RRs of OPEs associated with total indoor exposure (including dust intake, inhalation, and dermal absorption) using a modeling approach, and we found that the risk of TDtBPP is higher than most OPEs (Figure S12). The second scenario considers terrestrial exposure from food intake of herbivores, which was quantified using a comprehensive fate and exposure model called PROTEX (PROduction-To-EXposure), together with the measured concentrations of OPEs in outdoor air from Chicago (Figure S2).[33] In this scenario, the RR of TDtBPP is lower than that of TCEP but is 7–340 times higher than those of other traditional OPEs (Figure 4D). These relatively high risks associated with TDtBPP are driven by its higher toxicity and higher environmental concentrations in both indoor and outdoor environments. Given the persistent nature of TDtBPP (TDtBPP is more resistant to degradation across all environmental media and is more resistant to biotransformation compared with traditional OPEs) and the relatively high risks of TDtBPP, we propose that TDtBPP be considered by jurisdictions around the world to be a CEC.

Implication for policymaking

The increasing concentrations of TDtBPP in Arctic air over the past two decades suggest that the pollution caused by the atmospheric transformations of non-persistent OPAs is a global issue not previously recognized by environmental protection agencies and chemical manufacturers. Combining the current (the Arctic, Antarctic, and megacities) and previously reported field measurement data, laboratory experiments (OPA chemical transformation and OPE biotransformation experiments), and in silico modeling, the results demonstrate the limitations of existing OPE regulations which focus on the OPEs used in commercial products but not considering those indirectly formed from the atmospheric transformation of OPAs. Given the high production volume of OPAs (up to 8.7×10^4 and 9.6×10^4 tons year^{-1} in the United States and China, respectively; see Figure S13), it is likely that a substantial fraction of the OPAs will be transformed to OPEs through O_3 oxidation and photochemical reactions during their residence time in the environment and/or in the manufacturing of plastics. The O_3 oxidation mechanism described in this work represents an important indirect source of environmental OPEs, particularly indoors. The indirect source is especially important for some OPEs such as TPHP whose antioxidant precursor TPHPi is produced in the United States at levels five times higher than that for TPHP (Figure S14). This implies that the contribution of TPHPi chemical transformations to environmental TPHP needs to be assessed. Including OPA transformations in the assessment of environmental OPEs is essential for achieving effective control of OPEs.

It should be noted that a fraction of OPAs within commercial products may have already been transformed to OPEs upon O_3 oxidation or photo-transformation during manufacturing and storage. In this case, new commercial products may contain both unreacted and oxidized OPAs. For example, high levels of TDtBPPi and TDtBPP were detected in new face masks,[37] both of which can be emitted into the environment. Therefore, environmental OPEs may arise from two different processes. First, OPAs in commercial products are emitted to the environment and then oxidized by oxidants (e.g., O_3), producing environmental OPEs. Second, OPAs are oxidized to OPEs during manufacturing and storage, and the resulting OPEs can be further released to the environment, producing environmental OPEs. Regardless, both processes highlight the key role of OPA transformation in the formation of environmental OPEs. Further study is warranted to illustrate the life cycle of OPA-containing commercial products; only then can an accurate assessment for the contribution of different transformation pathways to environmental OPEs be achieved.

In addition to the implication for OPE regulations, the OPA transformation chemistry emphasizes additional monitoring needs. For example, the novel TDtBPP is not measured in existing environmental contaminants monitoring networks,[7] despite their intent to track global and regional distributions of contaminants (including OPEs). The global environmental ubiquity of TDtBPP shown here, combined with its propensity to possess higher risks relative to the traditional OPEs, underscores the need to further investigate its environmental prevalence and toxicological properties. This study also highlights the value of sample banks such as the one used here for Arctic air monitoring dating back to 1994, which allows for retrospective analysis of environmental trends for CECs.

One potential limitation of this study is that we use the concentrations of an OPA-novel OPE pair to demonstrate the importance of OPA transformation chemistry. Note that the measured concentrations of novel OPEs are related to many factors, including OPA transformation chemistry, the emission sources, and the physiochemical properties of OPEs. Further study is needed to illustrate the impact of these factors on environmental OPEs.

Finally, we note that limited consideration is given to atmospheric chemical transformation within existing contaminant assessment frameworks.[38] However, there is historical precedent for the importance of atmospheric transformations in the case of perfluoroalkyl substances, i.e., atmospheric transformation of fluorotelomer alcohols can lead to the formation of perfluorocarboxylic acids,[39] a class of chemical that is currently regulated because of its health effect.[16] Together with the current OPA study, this highlights the need to include atmospheric transformations in the development of regulations for chemicals of concern.

EXPERIMENTAL PROCEDURES

Resource availability

Lead contact

Further information and requests for resources and reagents should be directed to and will be fulfilled by the lead contact, Jonathan P.D. Abbatt (jonathan.abbatt@utoronto.ca).

Materials availability

This study did not generate new unique materials.

Data and code availability

The raw data supporting the findings of this study are publicly available on Zenodo: https://zenodo.org/record/8149048. Software used in this study include OECD screening model: https://www.oecd.org/chemicalsafety/risk-assessment/oecdpovandlrtpscreeningtool.htm; PROTEX model: https://eas-e-suite.com; TEST: https://www.epa.gov/chemical-research/toxicity-estimation-software-tool-test; and OPERA: https://github.com/kmansouri/OPERA.

Arctic air measurement

To quantify trace levels of chemicals in the Arctic air, we deployed a super high volume sampler (SHVS; ~13,500 m^3) and a high-volume active air sampler (HVAAS; ~2000 m^3) from 1992 (SHVS) or 2015 (HVAAS) to the present.[21,40] This large air volume enables us to quantify many chemicals that occurred at low levels (pg m^{-3}). Each air sample was collected during a 7-day sampling period from the Alert Global Atmosphere Watch Observatory, Nunavut, Canada (82°30'01"N, 62°19'48"W, 200 m above sea level [a.s.l.]), and measurements are continuous and ongoing.[21] In the SHVS, a 20-cm glass fiber filter (GFF) and two polyurethane foam (PUF) plugs (20-cm diameter, 4-cm thickness) were used to collect the particle-phase and gas-phase chemicals separately. For HVAAS, each sampling was composed of a GFF and a cartridge containing two PUFs (2.5-inch diameter) and 5 g of XAD-2 (Supelpak-2; Sigma Aldrich) inside the two PUFs. The particle-bound target compounds in the GFF were extracted by AirZone One Ltd (Mississauga, Canada) as described previously.[21] The extracts were split into two equal portions: one was archived, and the other was used for routine analysis. The impact of OPE degradation in the archived extracts is negligible, given that the extracts were stored at −20°C. The analytes were analyzed using an ultra-performance liquid chromatography coupled with a Xevo TQ-S triple-quadrupole mass spectrometer (Waters, Boston, MA, USA) using the optimized multiple reaction monitoring (MRM; see Table S5) mode.

The quality assurance measures included the analysis of representative samples of unused sampling materials (GFFs) from the field and the laboratory, repeat analysis of 1 in 10 samples, inclusion of cleanup recovery and internal standards in each sample extract, analysis of standard reference materials from the EPA repository, as well as routine participation in inter-laboratory round-robin testing programs and specialized inter-laboratory comparisons. For a chemical to be detectable, the sample must have exceeded the method quantification limit (MQL; pg m^{-3}), defined as MQL = mean blank + 3 × standard deviation (SD) of the blanks (Table S6). For chemicals not detected in the blank samples, the MQL was defined as the amount of chemical (pg) in the lowest standard, which gives a signal-to-noise ratio of 10 divided by the average sampling volume. Values below MQL were considered as non-detects and were replaced with 1/2 MQL when performing statistical analysis. The field measurement results of novel OPEs are shown in Table S7 and Note S3.

Antarctic air measurement

Air particle samples were collected at the Antarctic Great Wall Station of China (62°12′59″S, 58°57′52″W), using a total suspended particulate sampler (TSP; flow rate, 1.05 m^3 min^{-1}; TH-1000H; Wuhan Tianhong) with GFF filters (23 × 18 cm^2). Air samples (n = 8) were collected from January 11, 2020, to March 21, 2020, and from November 28, 2020, to January 23, 2021. The collected samples were wrapped in aluminum foil and stored at −20°C until analyzed.

Eight 1.8-cm^2 filter punches from each GFF filter were used to conduct the OPE and OPA analysis. Each filter was added to a pre-cleaned glass vial, extracted with 30 mL of acetonitrile containing 20 ng of internal standards (tris(2-chloroisopropyl) phosphate [TCPP]-d18, TCEP-d12, and tricresyl phosphate [TCP]-d21) in an ultrasonication bath for 30 min and centrifuged at 5,000 rpm for 5 min; the supernatant was transferred to another glass vial. The above extraction procedures were carried out three times for each sample. The extract was then dried under nitrogen gas and dissolved in 0.5 mL of methanol. Finally, the extract was vortexed for 2 min and filtered with a 0.22-μm membrane to remove insoluble materials. OPEs and OPAs were analyzed using an ultra-high-performance liquid chromatograph coupled to a triple-quadrupole mass spectrometer (UPLC-MS/MS; AB Sciex).

Toronto air measurement

Samples were collected at Highway 401W, 125 Resources Road, Toronto, Ontario, Canada (43°42'40"N, 79°32'35"W) from January to February 2018, under Canada's National Air Pollution Surveillance (NAPS) program. A modified HVAAS built by Environment and Climate Change Canada was used to collect particle-phase (PM_{30}) and gas-phase chemicals. Ambient air (~720 m^3) was drawn, over a period of 24 h, through a cartridge containing a Teflon-coated borosilicate GFF (20.32 × 25.40 cm) followed by a pair of PUF sorbent plugs (8.26 × 7.62 cm). Samples were collected once every 6 days with the cartridge remaining in the high-volume sampler between collection events. The filters and PUFs were wrapped in aluminum foil and stored at −10°C prior to extraction.

A Soxhlet apparatus was used to extract the samples using 350 mL of a 10:1 dichloromethane/acetone mixture for a period of 20–24 h. The resulting extracts were roto-evaporated to 5 mL and split into two equal portions. One portion was used for routine analysis, and the other portion was stored at ~4°C. The sample extracts were dried under a blow of nitrogen and dissolved in methanol, which was then analyzed by an UPLC-MS/MS (Waters, Boston, MA, USA).

Guangzhou indoor dust measurement

Indoor dust samples (n = 25) were collected in Guangzhou, China, from July to August 2021. Indoor dust samples were obtained by a vacuum cleaner (ZMO1550; Electrolux, Stockholm, Sweden) with a paper collector bag inserted into the nozzle. After vacuuming the floors of each dwelling's living room and bedrooms, each paper bag was detached and wrapped with pre-cleaned aluminum foil. Then the dust samples were sieved with a particle size <150 μm and were stored at −20°C in an amber glass jar prior to sample analysis.

The indoor dust samples were prepared by ultrasonic extraction with acetonitrile. In brief, a 50-mg sample was spiked with 50 ng of internal standards (TCEP-d12, TCPP-d18, tris(1,3-dichloro-2-propyl) phosphate [TDCPP]-d15, TPHP-d15, tris(2-ethylhexyl) phosphate [TEHP]-d51, TCP-d21, and tris(2-butoxyethyl) phosphate [TBEP]-d27) and transferred into a 10-mL glass centrifuge tube. Samples were extracted with 3 mL of acetonitrile by vortexing for 10 min and ultrasonication for 10 min. Following centrifugation at 4,500 rpm (2,081 × *g*) for 10 min, the supernatant was transferred to another glass tube. The extraction operation was repeated thrice, and the combined supernatants were concentrated to 5 mL under gentle nitrogen. Then, an aliquot of 1 mL of the extract was taken and filtered through a 0.22-μm filter member before instrumental analysis. OPEs and OPAs were analyzed using an UPLC-MS/MS (AB Sciex).

Heterogeneous O_3 reaction experiments

The heterogeneous reactions between gaseous O_3 and OPAs (TCEPi, TPHPi, and TDtBPPi) coated on circular microscope cover glasses (18-mm diameter) were studied using a dark FlowTube reactor described previously[41] and in Figure S4. A 100 μL aliquot of OPA solution (12.5, 9.6, and 6.4 μM for TCEPi, TPHPi, and TDtBPPi in methanol, respectively) was pipetted onto a cover glass, resulting in an average OPA coating thickness of ~1 nm after the evaporation of methanol in zero air; it is unlikely that the coatings are uniform. Fifteen OPA-coated cover glasses were aligned on a Teflon holder with an approximately 1.5-cm distance separation. The Teflon holder was placed inside the FlowTube reactor.

The total flow rate through the FlowTube reactor was 2 L min^{-1}. OPAs were exposed to 12–260 ppb of O_3 at 298 K. Different O_3 concentrations were used for different OPA experiments because of their different reactivity. The RH in the FlowTube was constantly maintained at a selected value (0% and 50% RH) by varying the ratio of dry to wet zero air. The O_3 concentration and RH were measured using an O_3 analyzer (Thermo, model 49i) and an RH sensor (VWR), respectively. To investigate the potential impact of air conditions (O_3 in zero air vs. O_3 in genuine indoor air) on the oxidation reactions of OPAs, TPHPi was also exposed to the genuine indoor air, which contained 25 ppb of O_3. At a given time point, the oxidized OPA samples were extracted with 1 mL of methanol containing BES (1 μM, used as internal standard) and analyzed using a Waters ultra-high-performance liquid chromatograph interfaced with a Xevo triple-quadrupole mass spectrometer.

The heterogeneous second-order reaction rate constants (*k*; cm^3 $molecule^{-1}$ s^{-1}) were calculated by measuring the decay of OPAs (Figure 3). The *k* can be determined using Equation 1:

$$\ln\frac{[OPA]_t}{[OPA]_0} = -k[O_3]t, \quad \text{(Equation 1)}$$

where $[OPA]_0$, $[OPA]_t$, $[O_3]$, and *t* are the initial mass of OPA (ng), the measured mass of OPA (ng) at a given O_3 exposure time, O_3 concentration (molecules cm^{-3}), and O_3 exposure time (s), respectively.

Although the mass of OPAs decreased considerably with increasing O_3 exposure time, the corresponding OPEs were simultaneously formed. We calculate the formation yields (%) of OPEs according to Equation 2:

$$\text{Formation yield}\ (\%) = \frac{n_{OPE}}{\Delta n_{OPA}} \times 100\%, \quad \text{(Equation 2)}$$

where n_{OPE} is the amount of formation product OPE (mol; measured with the UPLC-MS), and Δn_{OPA} is the differential amount of reactant OPA (mol; initial OPA − the remaining OPA).

Biotransformation experiments

Liver S9 incubation

In vitro metabolism of OPEs by Sprague Dawley rat liver S9 was conducted in triplicates. TDtBPP (10 nmol) was added to a glass vial, after which phosphate buffer (240 μL, 1 mol L^{-1}, pH 7.4) and NADPH regeneration solution (A: 50 μL, B: 10 μL) were added. The biodegradation was started by addition of rat liver S9, with final protein concentration of 1 mg mL^{-1}. Biodegradation of TPHP was conducted under the same conditions, which was used as the positive control. Negative control was conducted on OPEs in the above incubation system without liver S9. Blank control was conducted without OPEs addition in the S9 incubation system. The biodegradations were stopped by addition of 3.5 mL of methanol (containing TPHP-d15 and DPHP-d10). The mixture was then vortexed and centrifuged with supernatant for instrumental analysis.

Rat metabolism study

The rat metabolism study of OPEs was conducted under the approval from the Animal Care Committee at the University of Toronto. Seven-week-old male Sprague Dawley rats (n = 11) were divided into three groups: TDtBPP group (n = 5), TPHP group (positive control, n = 4), and blank control group (n = 2). The rats were administrated with chemicals (20 mg mL^{-1} dissolved in corn oil) via intraperitoneal (i.p.) injection at 2.5 mL kg^{-1}. The final administration level was 50 mg kg^{-1}. The blank control rats were dosed with clean corn oil. The chemical administration was conducted in two separate parts. In part one, urine and feces were collected whenever found by housing the rats on LabSand (Braintree Scientific) for 8 h a day. The urine and feces collected from each rat on each single day were put together to generate a single pooled urine and feces sample daily, respectively. In part two, we re-administrated the rats 21 days after the last sampling in part one. All rats were then euthanized 24 h after re-administration, after which rat blood and liver were sampled.

Before sample extraction, internal standards (TPHP-d15 and DPHP-d10) were added. Rat urine (0.2 mL) and blood samples (50 μL) were mixed with 0.8 and 0.45 mL of methanol, respectively, which were then sonicated and centrifuged with supernatant for instrumental analysis. Feces samples (0.2 g) were mixed with 4 mL of methanol and then sonicated. Acetone (4 mL) was used to extract rat liver samples (0.4 g), after which 1 mL of the extract was transferred and solvent exchanged to methanol. The sorbent of octadecyl silane C18 (0.2 g) was then added to the sample dissolved in methanol to absorb interferences prior to instrumental quantification.

Instrumental analysis

The target chemicals were analyzed using an ultra-high-performance liquid chromatograph interfaced with a Xevo triple-quadrupole mass spectrometer (Waters, Milford, MA, USA), with an ACQUITY BEH C18 (2.1 × 100 mm, 1.7 μm) as the separation column. Electrospray ionization (ESI) was performed in positive mode for OPEs and BDtBPP. Methanol and H_2O, both containing 0.1% of formic acid, were used as the mobile phases. Details can be found in the previous study.[42] For the analysis of DPHP, the ESI was performed in negative mode, while ammonium acetate (10 mmol L^{-1}) was used in the mobile phases. TPHP and DPHP were corrected by their internal standards. Concentrations of TDtBPP and BDtBPP in rat samples were measured by matrix-matched calibration. Recoveries of the TDtBPP, TPHP, and their metabolites ranged from 53% to 115%. No contamination of OPEs or metabolites was detected in the procedural blanks.

In silico modeling

The environmental persistence of OPEs was evaluated based on P_{ov} (overall persistence; days), a metric defined to characterize the average time that a chemical resides in an environmental system with multiple environmental media (soil, water, and air). The P_{ov} was estimated with the OECD persistence and long-range transport screening model (denoted OECD screening model).[32] As the model input, partitioning properties were estimated using BIOVIA COSMOtherm (version 21.0), COSMOconfX (version 21.0), and TmoleX (version 21.0.1), a well-established quantum chemistry and thermodynamics-based software package following the COSMO-RS theory to calculate the octanol-water partitioning coefficients (K_{OW}), and Henry's Law Constant (K_H; Pa m^3 mol^{-1}), from which octanol-air (K_{OA}), and air-water (K_{AW}) partitioning coefficients were derived.[43] The COSMOtherm-predicted partitioning properties of OPEs are shown in Table S8. The estimated half-lives for the OPEs in air, water, and soil are shown in Table S9.

The biotransformation half-lives (days) of OPEs were estimated using the BCFBAF module of EPI Suite (Figure S15; Table S10).[44] The bioaccumulation model includes a quantitative structure-activity relationship (QSAR) that estimates the biotransformation half-lives normalized for a 10-g fish at 15°C based on experimental values of biotransformation half-lives of 632 chemicals. The estimated biotransformation half-lives and COSMOtherm-calculated K_{OW} of OPEs were used as input to the bioaccumulation model developed by Arnot and Gobas[45] for bioaccumulation factor (BAF; a metric used for quantifying the bioaccumulation potential of chemicals) calculations. BAF is defined as the ratio between wet-weight-based chemical concentrations in an organism and concentrations in water under conditions involving all the primary chemical uptake and elimination routes. We used the calculated BAF for the upper-trophic-level fish as endpoints for evaluating the bioaccumulation potentials of OPEs.

The toxicity of OPEs was evaluated using the Toxicity Estimation Software Tool (TEST, version 5.1) that predicts the dose of OPEs that can cause 50% of rats in a population to die after oral ingestion (LD_{50}).[46] A lower LD_{50} corresponds to a higher toxicity. As a suite of quantitative structure-activity relationships (QSARs), TEST estimates oral rat LD_{50} based on experimental data of 7,400 chemicals, including 7 (TCEP, TCPP, TDCPP, TPHP, TEHP, TCP, and TBEP) of the 12 OPEs evaluated in this study. For each of the 7,400 chemicals, 797 two-dimensional molecular descriptors were calculated from the chemical structure. We used the hierarchical clustering-based QSAR to estimate the oral rat LD_{50} for TDtBPP, TNPP, BBPDP, TiDeP, and EHDP. The uncertainty analysis of the *in silico* predicted environmental hazards is shown in Note S4.

To compare the risks among the OPEs, we derive the RR via Equation 3 by scaling *Risk*(*x*) (the risk of each OPE) to $Risk_{max}$ (the highest risk among the 12 OPEs we evaluated).

$$R(x) = \frac{Risk(x)}{Risk_{max}} \quad \text{(Equation 3)}$$

The risk of a chemical refers to a negative effect caused by a particular exposure route to a chemical and can be quantified using Equation 4 as the quotient of chemical exposure (chemical intake rate [CIR]; mol d^{-1}] and the tolerable daily intake (TDI; mol d^{-1}):

$$Risk(x) = \frac{CIR(x)}{TDI(x)} = \frac{IR \times C(x)}{CF \times LD_{50}(x)}. \quad \text{(Equation 4)}$$

CIR can be calculated as the product of the intake rate (IR; kg d^{-1}) of a medium (e.g., dust or food) containing the chemical and the chemical's concentration (C; mol kg^{-1}) in the exposed medium. TDI is a toxicological-effect-related threshold above which the levels of exposure to humans or ecological organisms would cause adverse effects. TDI can be derived with a conversion factor (CF) applied to the toxicity endpoint (oral LD_{50}). The CF is related to body weight of the target organism and the uncertainty factor when extrapolating the toxicity endpoint from one target organism to another. The CF is assumed to be chemical independent. By combining Equations 3 and 4, the RR can be determined using Equation 5, which is directly related to the concentrations of OPEs in the exposed medium and LD_{50}:

$$RR(x) = \frac{\frac{IR}{CF}\frac{C(x)}{LD_{50}(x)}}{\max_i\left(\frac{IR}{CF}\frac{C(i)}{LD_{50}(i)}\right)} = \frac{\frac{C(x)}{LD_{50}(x)}}{\max_i\left(\frac{C(i)}{LD_{50}(i)}\right)}. \quad \text{(Equation 5)}$$

The RR of OPEs associated with indoor dust exposure was calculated with the measured OPE concentrations in indoor dust from Toronto (Figure S2). This

Toronto dataset was chosen because it is one of the most comprehensive indoor dust datasets that included the concentrations of both the novel and the traditional OPEs. Furthermore, we also calculated the risk associated with terrestrial food web exposures. Due to the lack of measured concentration data of both the novel and the traditional OPEs in the terrestrial food web, we took the measured OPE concentrations in the ambient air of Chicago (Figure S2) to constrain the OPE emissions to air using the urban module of the PROTEX model.[33] With emissions of a chemical to the environmental media, PROTEX is able to calculate the concentrations of the chemical in environmental compartments (e.g., air, water, soil, sediment), as well as in organisms in aquatic and terrestrial food webs. The input rate of emission of the OPEs to urban air was scaled to ensure the predicted air concentrations match the measurements. Then the model-predicted concentrations of OPEs in the terrestrial food web were used to estimate their RRs based on Equation 5. PROTEX is suited for defensible chemical assessments, given that it has been thoroughly evaluated against monitoring and biomonitoring data for a wide range of chemicals in various regional environments.[47]

SUPPLEMENTAL INFORMATION

Supplemental information can be found online at https://doi.org/10.1016/j.oneear.2023.08.004.

ACKNOWLEDGMENTS

We thank the Canadian Forces Station Alert for supporting data collection at the High Arctic Station of Alert. We thank David Harnish for help in securing Toronto air samples from the NAPS program of ECCC. Q.L. was supported by the National Natural Science Foundation of China (NSFC; 42275101). R. L. was supported by Shandong Provincial Natural Science Foundation, China (ZR2023JQ007). J.P.D.A. was supported by the Alfred P. Sloan Foundation (FG-2019-11404) and Natural Sciences and Engineering Research Council of Canada (NSERC; RGPIN-2017-05972). S.A.M. was supported by NSERC. X.Z. was supported by NSERC (DGECR-2021-00307). H.H. was supported by Crown-Indigenous Relations and Northern Affairs Canada's Northern Contaminants Program, with partial funding from the Government of Canada's Chemicals Management Plan. T.H. was supported by Government of Canada's Chemicals Management Plan. L.L. was supported by Environment and Climate Change Canada (GCXE22S061). Z.X. was supported by the NSFC (41941014) and Chinese Arctic and Antarctic Administration. L.Z. was supported by NSFC (22076064). Y.Z. was supported by NSFC (41977359). M.G. was supported by NSFC (42130606). This work does not reflect any regulatory conclusions for any substances mentioned.

AUTHOR CONTRIBUTIONS

Conceptualization, Q.L., R.L., J.P.D.A., and S.A.M.; methodology, Q.L., R.L., X.Z., J.P.D.A., S.A.M., H.H., and Z.X.; investigation, Q.L., R.L., X.Z., W.L., T.H., A.S., L.Z., P.L., H.L., F.Y., J.W., X.W., Y.Z., C.X., L.L., C.J., S.T., W.W., M.G., J.L., and S.-M.L.; supervision, Q.L., Z.X., H.H., J.P.D.A., and S.A.M.; software, X.Z., L.L., Y.Z., and C.J.; data curation, Q.L., R.L., X.Z., and W.L.; writing – original draft, Q.L., R.L., and X.Z.; writing – review & editing, Q.L., R.L., X.Z., H.H., J.P.D.A., and S.A.M.

DECLARATION OF INTERESTS

The authors declare no competing interests.

Received: December 17, 2022
Revised: April 26, 2023
Accepted: August 2, 2023
Published: August 25, 2023

REFERENCES

1. Escher, B.I., Stapleton, H.M., and Schymanski, E.L. (2020). Tracking complex mixtures of chemicals in our changing environment. Science *367*, 388–392.
2. United Nations (2022). The Sustainable Development Goals Report 2022.
3. European Commission (2020). Chemicals Strategy for Sustainability.
4. De Boer, J., and Stapleton, H.M. (2019). Toward fire safety without chemical risk. Science *364*, 231–232.
5. Blum, A., Behl, M., Birnbaum, L., Diamond, M.L., Phillips, A., Singla, V., Sipes, N.S., Stapleton, H.M., and Venier, M. (2019). Organophosphate ester flame retardants: are they a regrettable substitution for polybrominated diphenyl ethers? Environ. Sci. Technol. Lett. *6*, 638–649.
6. Xie, Z., Wang, P., Wang, X., Castro-Jiménez, J., Kallenborn, R., Liao, C., Mi, W., Lohmann, R., Vila-Costa, M., and Dachs, J. (2022). Organophosphate ester pollution in the oceans. Nat. Rev. Earth Environ. *3*, 309–322.
7. Saini, A., Harner, T., Chinnadhurai, S., Schuster, J.K., Yates, A., Sweetman, A., Aristizabal-Zuluaga, B.H., Jiménez, B., Manzano, C.A., et al. (2020). GAPS-megacities: A new global platform for investigating persistent organic pollutants and chemicals of emerging concern in urban air. Environ. Pollut. *267*, 115416.
8. US Environmental Protection Agency (2019). Initiation of Prioritization Under the Toxic Substances Control Act.
9. European Union (2019). Commission Regulation (EU) 2019/2021 of 1 October 2019 Laying Down Ecodesign Requirements for Electronic Displays Pursuant to Directive 2009/125/EC of the European Parliament and of the Council.
10. Government of Canada (2021). Risk Management Scope for TPHP, BPDP, BDMEPPP, IDDP, IPPP and TEP.
11. Wei, G.L., Li, D.Q., Zhuo, M.N., Liao, Y.S., Xie, Z.Y., Guo, T.L., Li, J.J., Zhang, S.Y., and Liang, Z.Q. (2015). Organophosphorus flame retardants and plasticizers: sources, occurrence, toxicity and human exposure. Environ. Pollut. *196*, 29–46.
12. Venier, M., Stubbings, W.A., Guo, J., Romanak, K., Nguyen, L.V., Jantunen, L., Melymuk, L., Arrandale, V., Diamond, M.L., and Hites, R.A. (2018). Tri (2, 4-di-t-butylphenyl) phosphate: a previously unrecognized, abundant, ubiquitous pollutant in the built and natural environment. Environ. Sci. Technol. *52*, 12997–13003.
13. Liu, R., and Mabury, S.A. (2019). Organophosphite antioxidants in indoor dust represent an indirect source of organophosphate esters. Environ. Sci. Technol. *53*, 1805–1811.
14. Shi, J., Xu, C., Xiang, L., Chen, J., and Cai, Z. (2020). Tris (2, 4-di-tert-butylphenyl) phosphate: an unexpected abundant toxic pollutant found in $PM_{2.5}$. Environ. Sci. Technol. *54*, 10570–10576.
15. Rottem, S.V. (2017). The use of arctic science: POPs, Norway and the Stockholm Convention. Arctic Rev. *8*. https://doi.org/10.23865/arctic.v8.723.
16. United Nations (2004). Stockholm Convention.
17. Garnett, J., Halsall, C., Vader, A., Joerss, H., Ebinghaus, R., Leeson, A., and Wynn, P.M. (2021). High concentrations of perfluoroalkyl acids in Arctic seawater driven by early thawing sea ice. Environ. Sci. Technol. *55*, 11049–11059.
18. Hung, H., Katsoyiannis, A.A., Brorström-Lundén, E., Olafsdottir, K., Aas, W., Breivik, K., Bohlin-Nizzetto, P., Sigurdsson, A., Hakola, H., Bossi, R., et al. (2016). Temporal trends of Persistent Organic Pollutants (POPs) in arctic air: 20 years of monitoring under the Arctic Monitoring and Assessment Programme (AMAP). Environ. Pollut. *217*, 52–61.
19. Liu, X., Chen, D., Yu, Y., Zeng, X., Li, L., Xie, Q., Yang, M., Wu, Q., and Dong, G. (2020). Novel organophosphate esters in airborne particulate matters: occurrences, precursors, and selected transformation products. Environ. Sci. Technol. *54*, 13771–13777.
20. Zhang, Q., Li, X., Wang, Y., Zhang, C., Cheng, Z., Zhao, L., Li, X., Sun, Z., Zhang, J., Yao, Y., et al. (2021). Occurrence of novel organophosphate esters derived from organophosphite antioxidants in an e-waste dismantling area: Associations between hand wipes and dust. Environ. Int. *157*, 106860.
21. Yu, Y., Katsoyiannis, A., Bohlin-Nizzetto, P., Brorström-Lundén, E., Ma, J., Zhao, Y., Wu, Z., Tych, W., Mindham, D., Sverko, E., et al. (2019).

Polycyclic aromatic hydrocarbons not declining in Arctic air despite global emission reduction. Environ. Sci. Technol. *53*, 2375–2382.

22. United Nations (2019). Frontier Technology Quarterly: Frontier Technologies for Addressing Plastic Pollution.
23. Yang, Y., Hu, C., Zhong, H., Chen, X., Chen, R., and Yam, K.L. (2016). Effects of ultraviolet (UV) on degradation of Irgafos 168 and migration of its degradation products from polypropylene films. J. Agric. Food Chem. *64*, 7866–7873.
24. Martin, P., Tuazon, E.C., Atkinson, R., and Maughan, A.D. (2002). Atmospheric gas-phase reactions of selected phosphorus-containing compounds. J. Phys. Chem. A *106*, 1542–1550.
25. Razumovskii, S.D., and Mendenhall, G.D. (1973). The rate constants for the reactions of ozone with triphenylphosphite and triphenylphosphine. Can. J. Chem. *51*, 1257–1259.
26. Weschler, C.J., and Carslaw, N. (2018). Indoor chemistry. Environ. Sci. Technol. *52*, 2419–2428.
27. Goldstein, A.H., Nazaroff, W.W., Weschler, C.J., and Williams, J. (2021). How do indoor environments affect air pollution exposure? Environ. Sci. Technol. *55*, 100–108.
28. Abbatt, J.P.D., and Wang, C. (2020). The atmospheric chemistry of indoor environments. Environ. Sci. Process. Impacts *22*, 25–48.
29. Forkel, R., Balzarini, A., Baró, R., Bianconi, R., Curci, G., Jiménez-Guerrero, P., Hirtl, M., Honzak, L., Lorenz, C., Im, U., et al. (2015). Analysis of the WRF-Chem contributions to AQMEII phase2 with respect to aerosol radiative feedbacks on meteorology and pollutant distributions. Atmos. Environ. X. *115*, 630–645.
30. Helmig, D., Oltmans, S.J., Carlson, D., Lamarque, J.-F., Jones, A., Labuschagne, C., Anlauf, K., and Hayden, K. (2007). A review of surface ozone in the polar regions. Atmos. Environ. X. *41*, 5138–5161.
31. European Environment Agency (1998). Tropospheric Ozone in EU-The Consolidated Report.
32. Wegmann, F., Cavin, L., MacLeod, M., Scheringer, M., and Hungerbühler, K. (2009). The OECD software tool for screening chemicals for persistence and long-range transport potential. Environ. Model. Softw. *24*, 228–237.
33. Li, L., Arnot, J.A., and Wania, F. (2018). Revisiting the contributions of far- and near-field routes to aggregate human exposure to polychlorinated biphenyls (PCBs). Environ. Sci. Technol. *52*, 6974–6984.
34. Cousins, I.T., Ng, C.A., Wang, Z., and Scheringer, M. (2019). Why is high persistence alone a major cause of concern? Environ. Sci. Process. Impacts *21*, 781–792.
35. World Meteorological Organization (2014). Scientific Assessment of Ozone Depletion.
36. Ma, J., Hung, H., Tian, C., and Kallenborn, R. (2011). Revolatilization of persistent organic pollutants in the Arctic induced by climate change. Nat. Clim. Change. *1*, 255–260.
37. Liu, R., and Mabury, S.A. (2021). Single-use face masks as a potential source of synthetic antioxidants to the environment. Environ. Sci. Technol. Lett. *8*, 651–655.
38. Liu, Q., Li, L., Zhang, X., Saini, A., Li, W., Hung, H., Hao, C., Li, K., Lee, P., Wentzell, J.J.B., et al. (2021). Uncovering global-scale risks from commercial chemicals in air. Nature *600*, 456–461.
39. Ellis, D.A., Martin, J.W., De Silva, A.O., Mabury, S.A., Hurley, M.D., Sulbaek Andersen, M.P., and Wallington, T.J. (2004). Degradation of fluorotelomer alcohols: a likely atmospheric source of perfluorinated carboxylic acids. Environ. Sci. Technol. *38*, 3316–3321.
40. Fellin, P., Dougherty, D., Barrie, L.A., Toom, D., Muir, D., Grift, N., Lockhart, L., and Billeck, B. (1996). Air monitoring in the Arctic: results for selected persistent organic pollutants for 1992. Environ. Toxicol. Chem. *15*, 253–261.
41. Zhou, Z., Zhou, S., and Abbatt, J.P.D. (2019). Kinetics and condensed-phase products in multiphase ozonolysis of an unsaturated triglyceride. Environ. Sci. Technol. *53*, 12467–12475.
42. Liu, R., and Mabury, S.A. (2018). Unexpectedly high concentrations of a newly identified organophosphate ester, tris (2, 4-di-tert-butylphenyl) phosphate, in indoor dust from Canada. Environ. Sci. Technol. *52*, 9677–9683.
43. Klamt, A., Eckert, F., and Arlt, W. (2010). COSMO-RS: an alternative to simulation for calculating thermodynamic properties of liquid mixtures. Annu. Rev. Chem. Biomol. Eng. *1*, 101–122.
44. US Environmental Protection Agency (2012). Estimation Programs Interface Suite™ v 4.11.
45. Arnot, J., and Gobas, F. (2003). A generic QSAR for assessing the bioaccumulation potential of organic chemicals in aquatic food webs. QSAR Comb. Sci. *22*, 337–345.
46. US Environmental Protection Agency (2020). User's Guide for T.E.S.T. (Toxicity Estimation Software Tool, Version 5.1): A Program to Estimate Toxicity from Molecular Structure.
47. Li, L., Hoang, C., Arnot, J.A., and Wania, F. (2020). Clarifying temporal trend variability in human biomonitoring of polybrominated diphenyl ethers through mechanistic modeling. Environ. Sci. Technol. *54*, 166–175.